J Intell Robot Syst (2013) 72:287–300
DOI 10.1007/s10846-012-9807-1

Optimal Trajectory Planning for Flexible Link Manipulators with Large Deflection Using a New Displacements Approach

H. R. Heidari · M. H. Korayem · M. Haghpanahi · V. F. Batlle

Received: 21 November 2011 / Accepted: 18 December 2012 / Published online: 16 January 2013

Abstract The main objective of the present paper is to determine the optimal trajectory of very flexible link manipulators in point-to-point motion using a new displacement approach. A new nonlinear finite element model for the dynamic analysis is employed to describe nonlinear modeling for three-dimensional flexible link manipulators, in which both the geometric elastic nonlinearity and the foreshortening effects are considered. In comparison to other large deformation formulations, the motion equations contain constant stiffness matrix because the terms arising from geometric elastic nonlinearity are moved from elastic forces to inertial, reactive and external forces, which are originally nonlinear. This makes the formulation particularly efficient in computational terms and numerically more stable than alternative geometrically nonlinear formulations based on lower-order terms. In this investigation, the computational method to solve the trajectory planning problem is based on the indirect solution of open-loop optimal control problem. The Pontryagin's minimum principle is used to obtain the optimality conditions, which is lead to a standard form of a two-point boundary value problem. The proposed approach has been implemented and tested on a single-link very flexible arm and optimal paths with minimum effort and minimum vibration are obtained. The results illustrate the power and efficiency of the method to overcome the high nonlinearity nature of the problem.

Keywords Flexible link · Finite element method · Large deflection · Path planning · Optimal control · Pontryagin

Part of this research was sponsored by the Spanish Government Research Program with the project DPI2012-37062-C02-01 (MINECO) and by the European Social Fund.

H. R. Heidari (✉)
Robotic Research Laboratory, College of Mechanical Engineering, Malayer University, Malayer, Iran
e-mail: hr_heidari@iust.ac.ir

M. H. Korayem · M. Haghpanahi
Robotic Research Laboratory, College of Mechanical Engineering, Iran University of Science and Technology, Tehran, Iran

V. F. Batlle
School of Industrial Engineering, University of Castilla La Mancha, 13071 Ciudad Real, Spain

1 Introduction

The research interest in flexible manipulator, i.e., light and large dimension robotic manipulator, has increased significantly during the last few years. Flexible manipulators have important application

in space exploration, manufacturing automation, construction, undersea, nuclear contaminated environments, and many other areas. Major advantages of flexible manipulator include, but not limited to, small mass, fast motion, and large force to mass ratio, which are reflected directly in the reduced energy consumption, increased productivity, and enhanced payload capacity. However, the use of structurally flexible robotic manipulators requires the inclusion of deformation effects due to flexibility in the dynamic equations which complicates the analysis and the control design. As a result, analysis of complex systems becomes impossible without using powerful computer-aided numerical methods. In this approach, a new nonlinear finite element model for the dynamic analysis is employed to describe nonlinear modeling for three-dimensional flexible link manipulators, in which both the geometric elastic nonlinearity and the foreshortening effects are considered. This formulation is particularly efficient in computational terms and numerically more stable than alternative geometrically nonlinear formulations based on lower-order terms. On the other hand, the cost reduction and increase of productivity are some of the most important goals of industrial automation. Therefore, to do an effective use of robotic systems, it is important to consider the path planning optimization of the system for a specific task. The dynamic behavior of the robot is of key importance in the task execution. Movements that may require high torque in the robot's joints shall not be implemented, due to technical limitations associated with the actuators. From the economic point of view, an important aspect is the energy required to perform a given task. As the movement will be executed repetitively, a strategy that optimizes energy consumption at each cycle of time may result in a significant cost reduction for long term applications. From a practical point of view, trajectory optimization for reducing vibration excitation in point-to-point maneuvers of flexible manipulators is also an important feature of path planning, since it increases the applicability of robotic systems. The open loop optimal control method is a suitable approach in the cases where the system has a large number of degree of freedom or optimization of the various objectives is targeted. Also, because of the offline nature of the open loop optimal control problem, many difficulties like system nonlinearities and all types of constraints may be considered and implemented easily.

Many approaches have been taken to the development of flexible link manipulators [1–3]. The dynamic model for links in most of these approaches has often based on rigid or small deflection theory but for applications like lightweight links, high-precision elements or high speed, it is necessary to capture the deflection caused by nonlinear terms.

Bakr presented a method for the dynamic analysis of geometrically nonlinear elastic robot manipulators. Geometric elastic nonlinearities are introduced into the formulation by retaining the quadratic terms in the strain-displacement relationships. This leads to the development of a new stiffness matrix which accounts for the combined effects of rotary inertia and shear deformation [4]. Simo and Vu-Quoc showed that for rotating structures, the appropriate accounting of the influence of centrifugal force on the bending stiffness and proposed a formulation based on the fully geometrically nonlinear beam theory. They demonstrated analytically the use of a first-order linear beam theory cannot account for the complete inertia effects to predict the influence of centrifugal stiffening [5]. Korayem and Basu derived an inverse dynamics and kinematics of a flexible manipulator in symbolic form based on the recursive Lagrangian assumed mode method [6]. Shaker and Ghosal considered nonlinear modeling of planar flexible manipulators with one and two revolute joints using the nonlinear finite element mathematical models. The motion equations of the systems are derived taking into account the nonlinear strain-displacement relationship [7]. Korayem and Heidari developed an algorithm for finding the maximum allowable dynamic load of flexible manipulators undergoing large deflection. A complete dynamic model is considered to characterize the motion of a compliant link capable of large deflection. The accuracy, actuator, and amplitude of residual vibration constraints and with imposing the maximum stress limitation as a new constraint are taken into account for the proposed algorithm during motion on a given trajectory [8].

Damaren and Sharf have presented and classified the different types of the inertial and geometric nonlinearities in the dynamics equation for flexible multibody systems. They observed that for sufficiently fast maneuvers of the flexible-link manipulators, the ruthlessly linearized approximation is wholly inadequate [9]. Mayo et al. derived the dynamic equations of flexible multibody systems considering complete geometrical nonlinearity. Their proposed formulation includes the effect of higher-order geometric elastic nonlinearity in the equations of the planar motion on bending displacements, while it is computationally very efficient. The stiffness terms in the motion equations generated by this formulation are exclusively limited to the constant stiffness matrix for the linear analysis [10].

Kane et al. investigated the beam undergoing large overall motions and reported that the conventional hybrid co-ordinate approach could lead to erroneous results such as prediction of dynamic softening of a rotating structure when dynamic stiffening is to be expected. Subsequently, many valuable researches on rotating beams had been done to modify the conventional hybrid coordinate approach in order to account for dynamic stiffening [11]. Absy and Shabana show that the effect of longitudinal displacement due to bending, in the equations of motion, would eliminate the third and higher order terms from the strain-energy expression if strain energy is written in terms of axial deformation. This has caused the nonlinear inertia terms and a constant stiffness matrix [12]. Omar and Shabana developed an isoparametric shear-deformable two-dimensional beam element based on the ANCF in which the elastic forces are determined using a general continuum mechanics approach. The use of the continuum mechanics approach leads to a simple expression for the elastic forces as compared to the use of local element frames. While the model accounts for the combined effects of shear deformation and rotary inertia, the finite element has zero Coriolis and centrifugal forces and leads to a constant mass [13].

On the other point of view, some researchers have studied the path planning problem for rigid and flexible manipulators. For instance, Wang et al. have solved the optimal control problem with direct method using the B-Spline functions in order to determine the maximum payload of a rigid manipulator [14]. Wilson et al. formulated path planning of a flexible manipulator as a discrete time open-loop optimal control problem, the solution of which is done via discrete dynamic programming [15]. Korayem and Nikoobin used the indirect solution of the optimal control problem to determine the DLCC of mobile manipulators. The Pontryagin's minimum principle is employed for path planning of mobile manipulators [16]. Mohri et al. have used indirect method for trajectory planning of mobile manipulators. They have proposed an approach to find the optimal path for both mobile base and manipulator links in order to achieve the minimum effort trajectory in point-to-point motion [17]. Park et al. considered the motion profiles of the joints as a Spline or polynomial functions. Then, the functions parameters are obtained in order to reduce the residual vibration of flexible manipulators at the end of the motion [18]. Benosman et al. investigated the problem of rest-to-rest motion of planar flexible manipulators and developed a simple method to realize joint motion between two equilibrium points over a desired time period as well as to prevent vibrations in the tips when the desired joint motions cease [19].

Szyszkowski and Youck used the optimal contro1 rule, based on rigid body dynamics, to minimize the time of a slewing maneuver of a single link. The influence of various flexibility parameters on the performance of the optimal control is investigated [20]. Sarkar et al. presented a systematic path planning technique to compute input torques off-line for a two-link flexible manipulator under gravity. Their method introduced two simple numerical algorithms to minimize end-point error for static case and tracking error for dynamic case [21]. Kojima et al. have proposed a technique that considers optimal trajectory planning method for residual vibration reduction of a two-link flexible robot arm and solves the optimal trajectory planning algorithm by using the genetic algorithm [22].

In this paper, first, the equations of motion are derived taking into account the nonlinear strain-displacement relationship using a new nonlinear finite element model for three-dimensional

dynamics analysis. Geometric elastic nonlinearities are introduced into the formulation by retaining the quadratic terms in the strain-displacement relationships. The strain energy is formulated in accordance with the slender beam theory and various non-linear terms are identified, in which both the geometric elastic nonlinearity and the foreshortening effects are considered. Then, an indirect solution of open-loop optimal control problem is used for path planning of flexible link manipulator. The necessary conditions for optimality are obtained from the Pontryagin's minimum principle, which is lead to a standard form of a two-point boundary value problem. Moreover by changing the penalty matrices values, one can obtain various optimal trajectories with minimum effort and minimum vibration. In order to verify the effectiveness of the new formulation, several experiments on a single-link very flexible arm has been carried out and the results are demonstrated the performance and merits of the proposed method.

2 Nonlinear Strain-Displacement Relationship

The analysis of flexible link can be modeled by slender elastic beams. In the classical formulations of beam elements, the beam cross section is assumed to remain rigid when the beam deforms. In Euler–Bernoulli beam theory, it is assumed that the beam cross section remains rigid and perpendicular to the beam centerline. In accordance with the assumptions of Euler-Bernoulli and neglect shear effects, the exact non-linear relationship for three-dimensional beam element of the Cauchy-Green strain tensor in terms of the displacement field is [23]:

$$\varepsilon_{xx} = \frac{\partial u}{\partial x} - y\,\frac{\partial^2 v}{\partial x^2} - z\,\frac{\partial^2 w}{\partial x^2} + \frac{1}{2}\left[\left(\frac{\partial v}{\partial x}\right)^2 + \left(\frac{\partial w}{\partial x}\right)^2\right] \tag{1}$$

where y and z are measured from the neutral axis of the beam and u, v, w denote the longitudinal and transverse displacements, respectively, at y = 0 and z = 0.

Assuming a linear stress-strain relationship, the potential energy can be obtained as

$$U = \frac{E}{2}\int_v \varepsilon_{xx}^2\, dV \tag{2}$$

Expanding the above integral, and since y is measured from the neutral axis, all integrals of the form $\int y\, dA$ must vanish, it takes the form:

$$\begin{aligned} U = {} & \frac{E\,A}{2}\int_0^l \left(\frac{\partial u}{\partial x}\right)^2 dx + \frac{E\,I}{2}\int_0^l \left(\frac{\partial^2 v}{\partial x^2}\right)^2 dx \\ & + \frac{E\,A}{2}\int_0^l \left(\frac{\partial u}{\partial x}\right) \times \left(\frac{\partial v}{\partial x}\right)^2 dx \\ & + \frac{E\,A}{2}\int_0^l \frac{1}{4}\left(\frac{\partial v}{\partial x}\right)^4 dx \\ & + \frac{E\,I}{2}\int_0^l \left(\frac{\partial^2 w}{\partial x^2}\right)^2 dx + \frac{E\,A}{2}\int_0^l \left(\frac{\partial u}{\partial x}\right) \\ & \times \left(\frac{\partial w}{\partial x}\right)^2 dx + \frac{E\,A}{2}\int_0^l \frac{1}{4}\left(\frac{\partial w}{\partial x}\right)^4 dx \\ & + \frac{E\,A}{4}\int_0^l \left(\frac{\partial v}{\partial x}\right)^2 \left(\frac{\partial w}{\partial x}\right)^2 dx \end{aligned} \tag{3}$$

where E, A, I, and l denote the Young's modulus, cross-sectional area, moment of inertia of the cross section, and length, respectively. In this investigation, a more efficient computationally model is developed, in which both the geometric elastic nonlinearity and the foreshortening effects are considered. The proposed formulation takes into account a distinction between the longitudinal displacement due to axial deformation, denoted as s, and the longitudinal displacement can occur due to the foreshortening effect, denoted by u_{fs} (Fig. 1). The longitudinal displacement caused by transverse deflection of the neutral axis of the beam can be expressed as [11]

$$u_{fs} = -\frac{1}{2}\int_0^x \left[\left(\frac{\partial v}{\partial x}\right)^2 + \left(\frac{\partial w}{\partial x}\right)^2\right] dx \tag{4}$$

The assumed field of displacements for $\mathbf{u}$ can be written as follow:

$$\mathbf{u} = \begin{bmatrix} u \\ v \\ w \end{bmatrix} = \begin{bmatrix} s + u_{fs} \\ v \\ w \end{bmatrix} \tag{5}$$

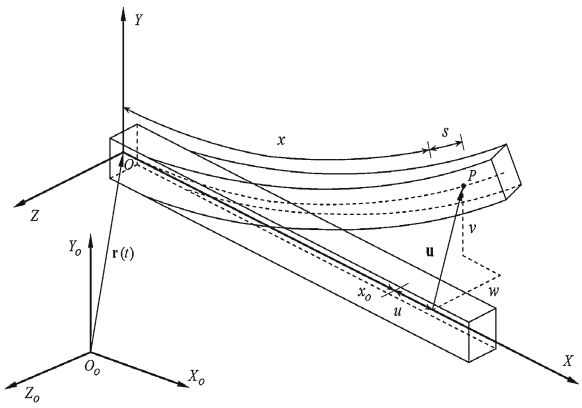

Fig. 1 Undeformed and deformed configurations of the Beam Element

If the general expression of the strain energy of Eq. 3 is rewritten in terms of s, v and w, leading to

$$U = \frac{E\,A}{2}\int_0^l \left(\frac{\partial s}{\partial x}\right)^2 dx + \frac{E\,I}{2}\int_0^l \left(\frac{\partial^2 v}{\partial x^2}\right)^2 dx + \frac{E\,I}{2}\int_0^l \left(\frac{\partial^2 w}{\partial x^2}\right)^2 dx \tag{6}$$

This formulation has caused the nonlinear inertia terms and a constant stiffness matrix in the motion equations. However, the proposed approach has exactly the same degree of approximation as classical formulation, but it is much more efficient computationally. The FEM will be utilized to discretize the flexible link. Each flexible link is assumed to be discretized into a finite number of beam elements, with each element consisting of two nodes with five degrees of freedom at each node as shown in Fig. 2.

The global position vector **r**, can be defined by appropriately considering the position vector of the corresponding local coordinate in the global reference system as follow

$${}^0_i r = {}^0_{i-1} r + [R] \begin{Bmatrix} x + s + u_{fs} \\ v \\ w \end{Bmatrix} \tag{7}$$

where $[R]$ is the transformation matrix. The flexural and axial deformations of any arbitrary point in the element can be described in terms of shape functions, **S** as

$$\begin{Bmatrix} s \\ v \\ w \end{Bmatrix} = \mathbf{S}\ \{q_i\}^T \tag{8}$$

The vector of nodal coordinates $\{q_i\}$ contains the displacements and slopes, for element "ij" of link i (Fig. 2). The shape functions **S** includes Hermitian shape function to derive the flexural deformations and linear shape function to approximate the axial deformations as follows

$$\mathbf{S} = \begin{bmatrix} N_1 & 0 & 0 & 0 & 0 & N_6 & 0 & 0 & 0 & 0 \\ 0 & N_{12} & 0 & N_{14} & 0 & 0 & N_{17} & 0 & N_{19} & 0 \\ 0 & 0 & N_{23} & 0 & N_{25} & 0 & 0 & N_{28} & 0 & N_{30} \end{bmatrix} \tag{9}$$

where the shape functions N_i are given by $\left(\xi = \frac{x}{l}\right)$

$$\begin{aligned} N_1 &= 1 - \xi, & N_6 &= \xi \\ N_{12,23} &= 1 - 3\xi^2 + 2\xi^3, & N_{14,25} &= \left(\xi - 2\xi^2 + \xi^3\right) l \\ N_{17,28} &= 3\xi^2 - 2\xi^3, & N_{19,30} &= \left(-\xi^2 + \xi^3\right) l \end{aligned} \tag{10}$$

The kinetic energy for the overall system is obtained by computing the kinetic energy for each element ij and then summing over all the elements. By derivative of Eq. 7, the global position vector of point **P** on the Euler–Bernoulli beam, the absolute velocity vector can be obtained.

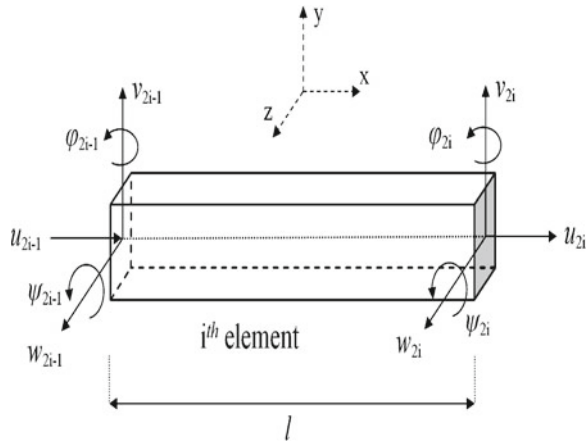

Fig. 2 The Beam Element with five degrees of freedom at each node

Using the absolute velocity vector can be defined the kinetic energy of the *ith* element of link as [8]

$$T = \frac{1}{2}\int_V \rho\, \dot{\mathbf{r}}^{\mathrm{T}}\, \dot{\mathbf{r}}\, dV \tag{11}$$

where V and ρ are the volume and the mass density of the beam element respectively.

The potential energy of element *ij* comprises two components, U_{gj} due to gravity and U_{ej} due to elasticity.

$$U_j = U_{gj} + U_{ej} \tag{12}$$

The gravitational potential energy of element '*ij*' of link becomes:

$$U_{gj} = \int_0^{l_1} \rho A\, g \begin{bmatrix} 0 & 0 & 1 \end{bmatrix} R \begin{Bmatrix} s \\ v \\ w \end{Bmatrix} dx_j \tag{13}$$

The strain energy for each beam element can be expressed using the strain vector ε and the constitutive equations, $\sigma = \mathbf{E}.\varepsilon$ as follows

$$U_{ej} = \frac{1}{2}\int_V \varepsilon^T . \mathbf{E} . \varepsilon\, dV = \frac{1}{2}\gamma_j^T\, K_j\, \gamma_j \tag{14}$$

where

$$\{\gamma_j\} = \begin{Bmatrix} s_{2i-1} & v_{2i-1} & w_{2i-1} & \varphi_{2i-1} & \psi_{2i-1} \\ s_{2i} & v_{2i} & w_{2i} & \varphi_{2i} & \psi_{2i} \end{Bmatrix} \tag{15}$$

The elastic constant of the material, $\mathbf{E}$ is defined for an isotropic homogenous material and $\mathbf{K_j}$ is stiffness matrix of beam element as follows

$$\mathbf{K_j} = \frac{E\,I}{l^3}\begin{bmatrix} Al^2/I & 0 & 0 & 0 & 0 & -Al^2/I & 0 & 0 & 0 & 0 \\ & 12 & 0 & 6l & 0 & 0 & -12 & 0 & 6l & 0 \\ & & 12 & 0 & 6l & 0 & 0 & -12 & 0 & 6l \\ & & & 4l^2 & 0 & 0 & -6l & 0 & 2l^2 & 0 \\ & & & & 4l^2 & 0 & 0 & -6l & 0 & 2l^2 \\ & & & & & Al^2/I & 0 & 0 & 0 & 0 \\ & & & & & & 12 & 0 & -6l & 0 \\ & & Sym. & & & & & 12 & 0 & -6l \\ & & & & & & & & 4l^2 & 0 \\ & & & & & & & & & 4l^2 \end{bmatrix} \tag{16}$$

Since flexible link comprises n elements, its total potential energy is:

$$U = \sum_{j=1}^{n} U_j = U_g + \frac{1}{2}\gamma^T\, \mathbf{K}\, \gamma \tag{17}$$

where $\mathbf{K}$ is the general stiffness matrix.

3 Dynamic Equations Governing the Motion

The Lagrangian method is utilized to formulate the dynamic equations governing the motion of the flexible manipulator systems. In order to derive dynamic equations, the kinetic energy and the potential energy are computed for the entire system. The kinetic energy for the overall system is obtained by computing the kinetic energy for each element *ij* and then summing over all the elements. Also, the potential energy of the manipulator is obtained by computing the strain energy for each element *ij* due to elasticity and gravity of any link.

After calculation these energies, by applying the Lagrangian procedure and performing some algebraic manipulations, the compact form of the governing equations of motion can be obtained from

$$\left[M\,(q)\right]\{\ddot{q}\} + \left[C\right]\{\dot{q}\} + [K]\{q\} + h\,(q, \dot{q}) = \tau \tag{18}$$

where $[M]$ is the nonlinear mass matrix, $[C]$ is the Structural damping matrix, $[K]$ is the stiffness matrix. $h\,(q, \dot{q})$ considers the contribution of other dynamic forces such as centrifugal, Coriolis and gravity forces while τ consists of generalized external forces/torques.

4 Optimal Motion Planning Problem

The path planning optimization of the robot for a specific task is of key importance in industrial automation. In this section, the off-line global

trajectory planning for flexible link manipulators in point-to-point motion is formulated as an optimization problem whose solution is obtained by using the optimal control method. The optimal control approach provides a powerful tool for designers to create various optimal paths via defining the proper performance measure. The computational method to solve the trajectory planning problem is based on the indirect solution of open-loop optimal control problem. The Pontryagin's minimum principle is applied to obtain the optimality conditions, which is lead to a standard form of a two-point boundary value problem. The optimal control can formally be presented as the minimization of the chosen cost or objective function specifying precisely the desired goal. The purpose of the optimal control problem is to determine the control $u(t)$ that minimizes the performance index $J(u)$. In this investigation, the specific objective functional J is to obtain the optimal paths with minimum effort and vibration, which can be written as [16]

$$Minimize\, J = \int_0^{t_f} L\left(X\left(t\right), U\left(t\right)\right) dt = \frac{1}{2}\left\|X_1\right\|_{W_P}^2 + \frac{1}{2}\left\|X_2\right\|_{W_V}^2 + \frac{1}{2}\left\|U\right\|_R^2 \tag{19}$$

where the integrand $L(.)$ is a smooth, differentiable function in the arguments, $X(t)$ and $U(t)$ denote the state space form of the generalized coordinate and the joint torque, respectively. $\|X\|_K^2 = X^T K X$ is the generalized squared norm, W_P, W_V are symmetric, positive semi-definite $(k \times k)$ weighting matrix and R is symmetric, positive definite $(k \times k)$ matrix. The designer can decide on the relative importance among the angular position, angular velocity, vibration's amplitude and control effort by the numerical choice of penalty matrices W_P, W_V and R. In order to minimize the objective function subjected to the nonlinear dynamic equations, the well-known Pontryagin minimum principle is used and by introducing the costate vector ψ, the Hamiltonian function of the system can be defined as:

$$H\left(X, U, \psi, t\right) = L\left(X, U\right) + \psi^T \dot{X} \tag{20}$$

The PMP then implies that a necessary condition for a local minimum is that H be minimized with respect to $u(t)$ at all times. If it is assumed that the set of admissible inputs is bounded $U_i^- \leq u_i^* \leq U_i^+$, this condition is equivalent to

$$\dot{X} = \partial H / \partial \psi,\ \dot{\psi} = -\partial H / \partial X,\ 0 = \partial H / \partial U \tag{21}$$

The boundary values can be expressed as:

$$X\left(t_i\right) = X_i,\ X\left(t_f\right) = X_f; \tag{22}$$

where $X(t_i)$ and $X(t_f)$ represent the positions and velocities of the links at the beginning and at the end of the maneuver. The optimal trajectory is then obtained by solving the $2n$ differential equations.

$$\begin{cases} \dot{x}^*\left(t\right) = \dfrac{\partial \mathrm{H}}{\partial p}\left(x^*\left(t\right), u^*\left(t\right), p^*\left(t\right), t\right) \\ \dot{p}^*\left(t\right) = -\dfrac{\partial \mathrm{H}}{\partial x}\left(x^*\left(t\right), u^*\left(t\right), p^*\left(t\right), t\right) \\ H\left(x^*\left(t\right), u^*\left(t\right), p^*\left(t\right), t\right) \leq H\left(x^*\left(t\right), u\left(t\right), p^*\left(t\right), t\right) \end{cases} \tag{23}$$

The set of dynamic equations, the governing optimal control problem and the boundary conditions are lead to a standard form of a two-point boundary value problem, which is solvable with numerical techniques such as shooting, collocation, and finite difference methods. In this study, bvp4c command in MATLAB® which is based on the collocation method is used to solve the obtained problem. The details of the numerical technique used in MATLAB® to solve the TP-BVP are given in [24]. The method iterates on the initial values of the costate until the final boundary conditions are satisfied by the following desired accuracy

$$h\left(X\left(t_f\right), t_f\right) = \frac{1}{2}\left\|X_1\left(t_f\right) - X_{1f}\right\|_{W_p}^2 + \frac{1}{2}\left\|X_2\left(t_f\right) - X_{2f}\right\|_{W_V}^2 \leq \varepsilon \tag{24}$$

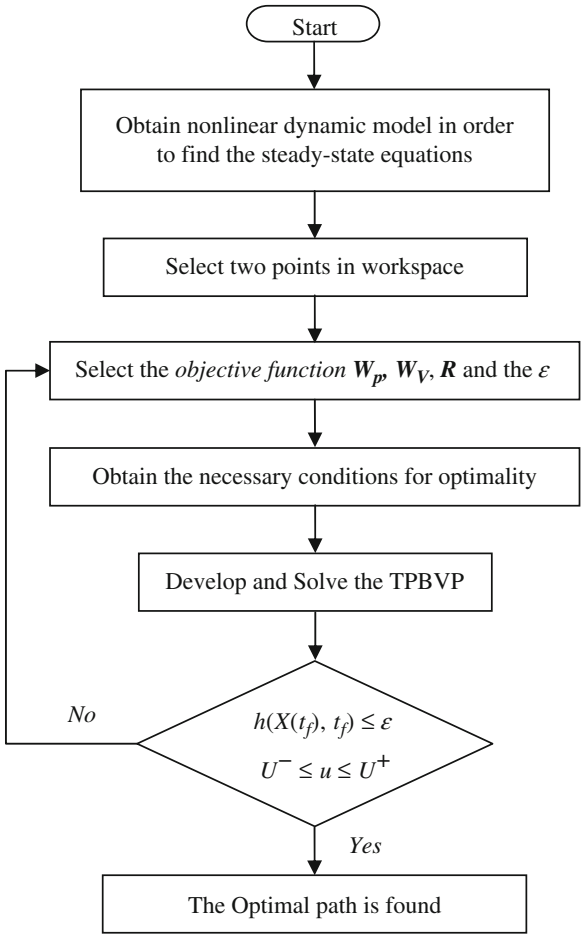

Fig. 3 Optimal path algorithm

Now, by using the solution of obtained TPBVP, an algorithm is presented in Fig. 3 in order to find the optimal paths.

5 Simulation and Experimental Results

In this section, numerical and experimental results are presented to show the validity and effectiveness of the geometrically nonlinear flexible link and computed the optimal trajectory in point-to-point motion. In order to initially check the validity of the proposed model, the spin-up manoeuvre problem is considered. A proper definition of beam deformation for the spinning beam demands coupling of the axial force with a bending moment. The capability of capturing this so-called geometrical or centrifugal stiffening effect is examined by modeling the rapidly spinning flexible beam in Fig. 4 using the parameters and angular displacements reported by Wu and Haug [25].

The beam has a length of 8 m, a width of $1.986e10^{-3}$ m, a height of $3.675e10^{-2}$ m, a Young's modulus of $6.895e10^{10}$ N/m^2 and a density of 2766.67 kg/m^3. The angular displacement $\theta(t)$ about the global Z axis is given as follows:

$$\theta = \begin{cases} \dfrac{\omega_s}{T_s}\left\{\dfrac{1}{2}t^2 + \left(\dfrac{T_s}{2\pi}\right)^2\left[\cos\left(\dfrac{2\pi t}{T_s}\right) - 1\right]\right\}, & t < T_s \\ \omega_s\left(t - \dfrac{T_s}{2}\right), & t \ge T_s \end{cases} \tag{25}$$

where $T_s = 15$ s and $\omega_s = 4$ rad/s. The computational results obtained with the proposed formulation using an implicit Runge—Kutta method for a simulation time of 20 s are illustrated in Fig. 5. The classical model [23] is made of 8 and 16 finite Euler–Bernoulli beam elements; the proposed model is discretized with 4 and 8 elements. It can be seen from the tip displacements given in Fig. 5 that the both models correctly capture the geometric stiffening effect, although the rate of convergence to the solution in the case of proposed model is better than that of classical model. Furthermore, the convergent solutions agree well with those given in the literature [25].

More surprisingly, significant saving in computer time was achieved using this model. It was observed that the proposed model is two times faster than the classical model.

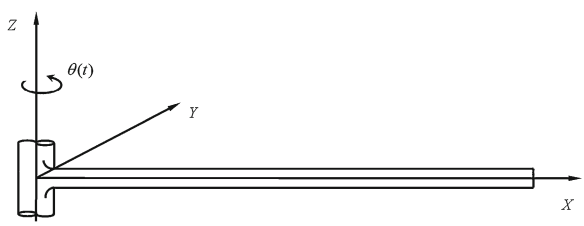

Fig. 4 Spin-up manoeuvre

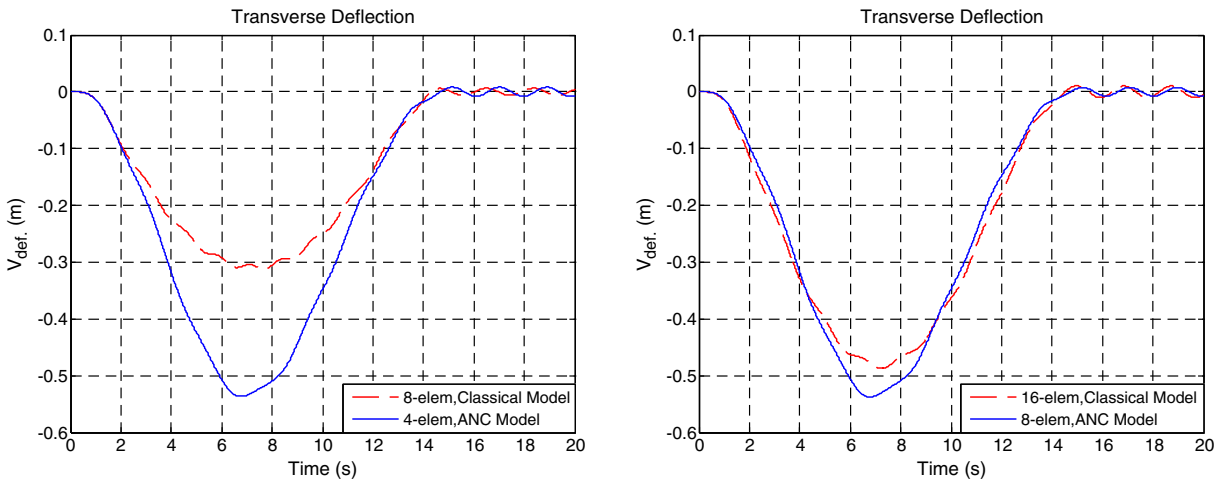

Fig. 5 Vertical tip deflection of the Classical Model (8 and 16 elements)—proposed Model (4 and 8 elements)

A useful indicator of the capability of capturing the geometrical stiffening effect is the steady-state axial extension of the beam. The exact solution for the beam axial extension u_x can be written in following form [5]:

$$u_x = L\left(\frac{\tan(a\,\omega_s)}{a\,\omega_s} - 1\right), \qquad a = \sqrt{\frac{\rho}{E}}L \tag{26}$$

The analytical value of the axial extension of the beam at steady-state phase in this case is 1.0957×10^{-4} m. As can be seen from Fig. 6, the steady-state axial extension of the beam corresponds to the analytical value with good accuracy.

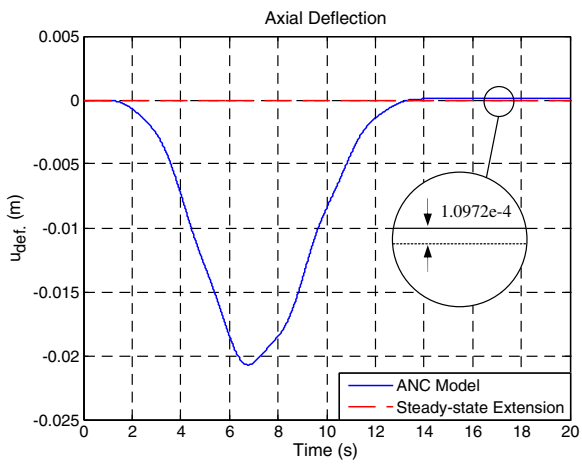

Fig. 6 The difference of the tip axial deflection between proposed model and the steady-state extension

Several simulations and experiments on a three-dimensional flexible link manipulator have been carried out to illustrate the performance of the proposed approach and have been obtained the optimal paths with minimum effort and minimum vibration. Figure 7 shows the flexible manipulator used for the experiments. The experimental platform is constructed of two DC motors, θ and ϕ rotations, that drive a flexible link made of carbon fiber as shown in Fig. 7. This configuration allows a spherical motion for flexible link. The flexible link can be changed with different lengths and diameters. The sensor systems consist of two incremental encoders for measuring the motors angle and a F/T sensor in order to estimate all six components of force and torque.

An Optotrak motion-measurement system with three infrared cameras is used to capture x, y and z coordinate data at a sampling rate of 120 Hz and precision 0.3 mm. An aluminum sphere at the tip of the flexible carbon fiber link acts as the payload. Simulation and experimental results of two case studies are presented to determine the extent to which the generated trajectory improves the actual performance of the manipulator with respect to other trajectories and the given objective functional.

Through the use of the model, the optimal trajectory is generated and compared, both in

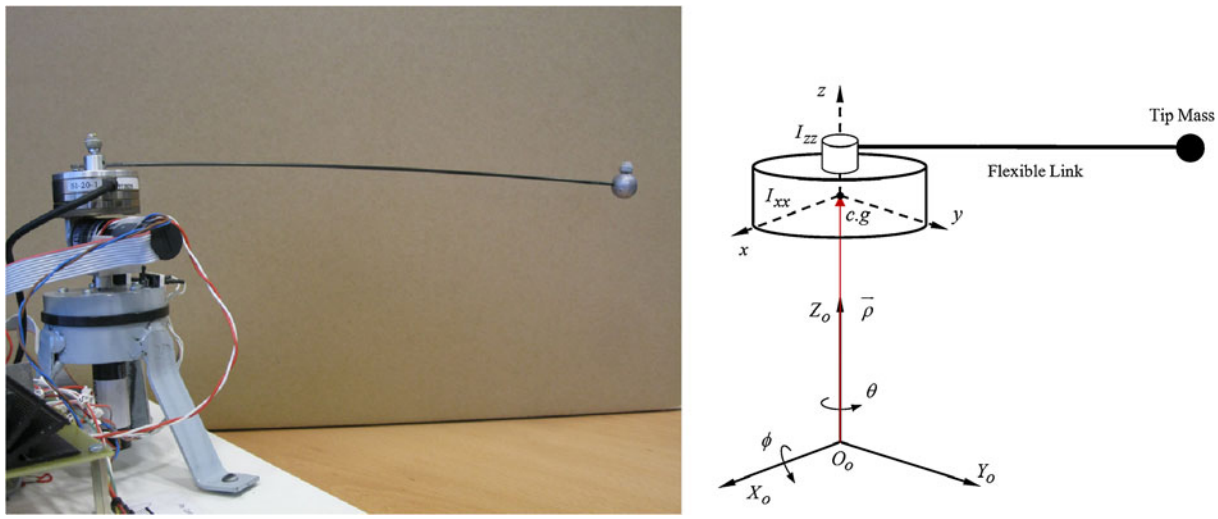

Fig. 7 Experimental setup and schematic view of the robot

simulation and experimentally, to a fourth-order polynomial trajectory designed in [26] in order to evaluate the results. One of the main advantages of this trajectory is that the tip vibrations reduce during robot maneuver, and achieving the fastest performance possible without saturating the motor. Also, the trajectory profile is symmetrical and invertible which the boundary conditions are zero velocity and acceleration at each end of the trajectory.

5.1 First Case Study: Optimal Path for Minimum Effort

The motion planning problem is to find the optimal trajectory with minimum effort. The path with minimum effort is a path in which the minimum torque is exerted by each motor in point-to-point motion. Therefore, penalty matrices can be considered as $R = diag\ (1)$ and $W_p = W_V = [0]$. This cost function is typical of systems that need to conserve energy during a particular operation. The parameters of the flexible manipulator are given in Table 1. The system is initially at rest, thus the initial conditions are $\theta(0) = 0$, $\phi(0) = 0$ (point **A** in Fig. 8). The final time is set to $t_f = 0.5\ s$ and the final conditions are $\theta(t_f) = 60°$, $\phi(t_f) = 40°$ (point **B** in Fig. 8) and also

Table 1 Physical properties of the flexible manipulator and payload

Parameter	Value	Unit
Length of links	$L = 0.3$	m
Link mass	$m_l = 1.44$	gram
Diameter	$D = 2 \times 10^{-3}$	m
Young's modulus of material	$E = 125 \times 10^9$	N/m^2
Tip mass	$m_t = 33.8$	gram

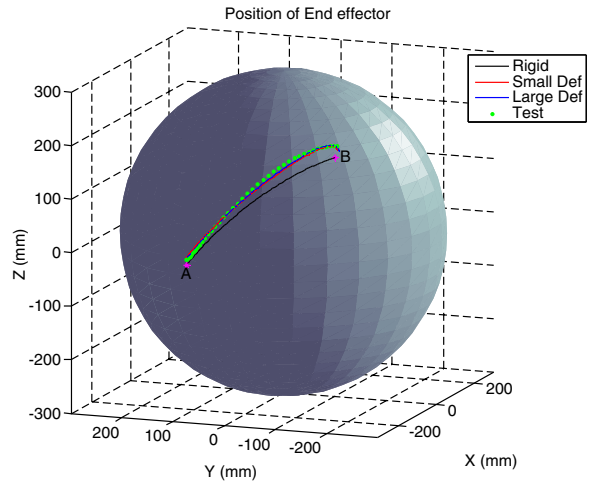

Fig. 8 The optimal paths between point **A** and **B** via minimum effort

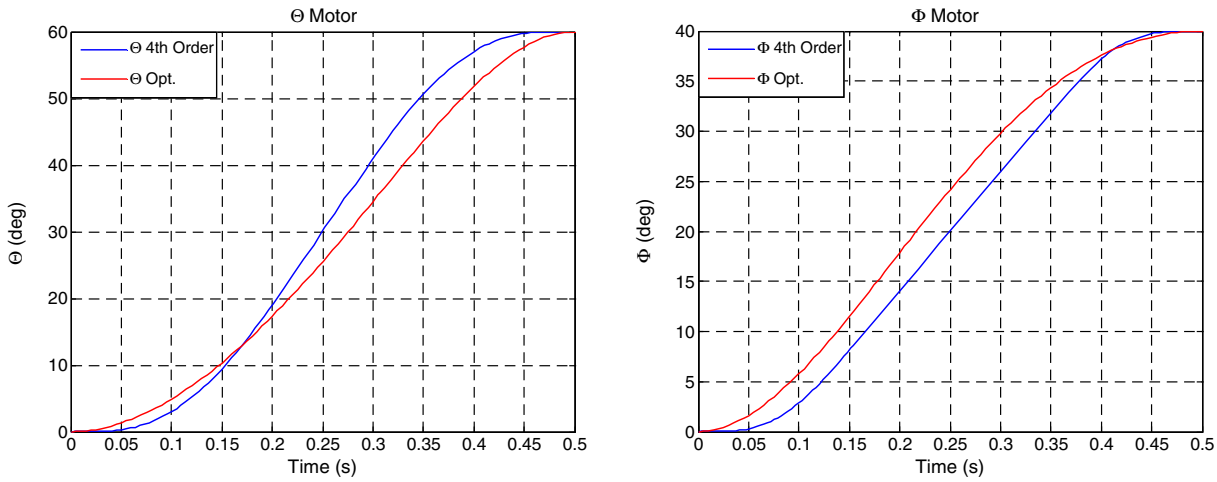

Fig. 9 The optimal angular positions of the θ and ϕ compared to fourth order trajectory

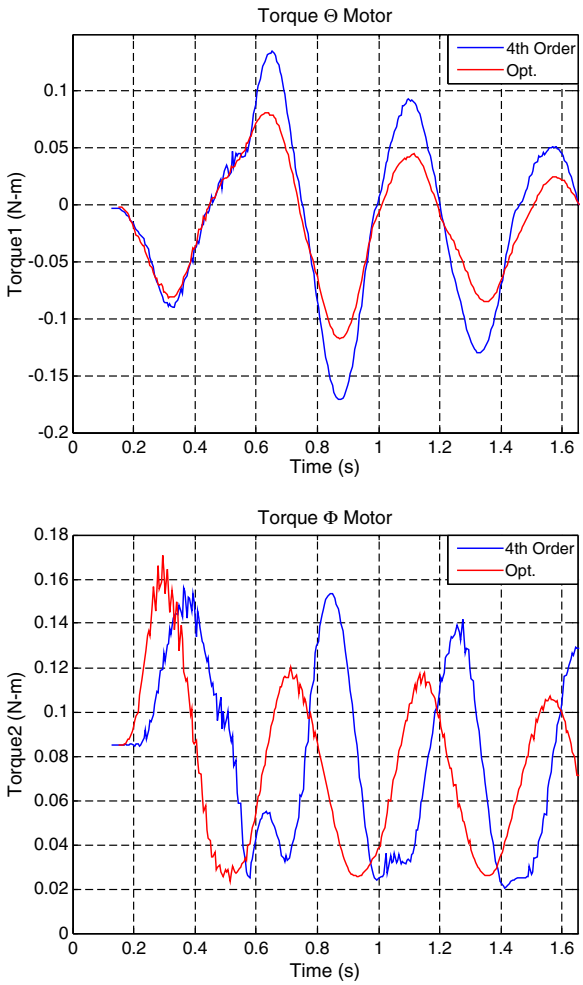

Fig. 10 Minimum effort of the θ and ϕ motors in comparison with fourth order trajectory

the remaining boundary conditions are equal to zero.

A comparative study is carried out between the simulation results (small and large models) and experimental result as shown in Fig. 8. The optimal angular positions of link, corresponding to the minimum effort are shown in Fig. 9. The experimental results presented in Fig. 10 show that the generated trajectory improves the actual performance of the manipulator actuators with respect to other trajectory. It can be seen, the

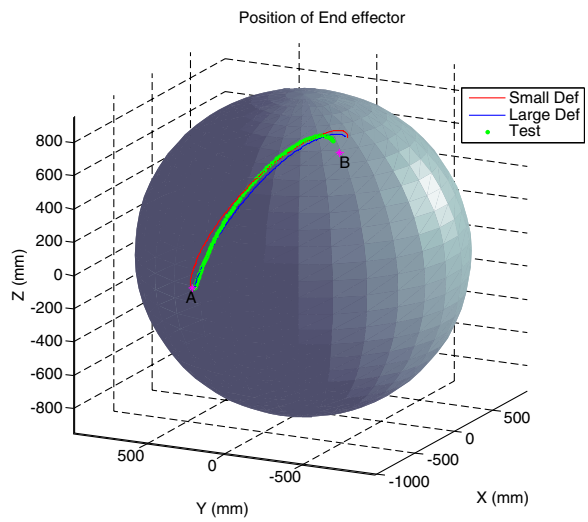

Fig. 11 The optimal paths between point **A** and **B** via minimum vibration

Table 2 Physical parameters used for second case study

Parameter	Value	Unit
Length of links	$L = 1$	m
Link mass	$m_l = 4.73$	gram
Diameter	$D = 2 \times 10^{-3}$	m
Young's modulus of material	$E = 125 \times 10^9$	N/m^2
Tip mass	$m_t = 5.74$	gram

flexibility of link will increase the oscillation of torque curves.

Although the solution trajectory exhibited some sensitivity to nonlinear modeling of flexible system, the interpretation of the optimal joint paths provided, corresponding to the minimum effort is relatively insensitive to variations in the flexible model parameters. The same optimal path would be expected for any flexible manipulator with different transverse bending stiffnesses.

5.2 Second Case Study: Minimum Vibration Trajectory

An important path planning problem for flexible manipulators studied by many researchers is to obtain the minimum vibration trajectory. The optimization objective is to minimize the vibration excitation during the motion. Hence, the proper penalty matrices are selected to be $R = diag\ (1)$ and $W_p = W_V = [10]$. The task is considered to move the joints from an initial point ($\theta(0) = 0°$, $\phi(0) = 0°$ point **A** in Fig. 11) to final configuration $\theta(t_f) = 45°$, $\phi(t_f) = 45°$ (point **B** in Fig. 11) for a rest-to-rest maneuver during the overall time $t_f = 1$ s. Table 2 lists the physical properties of the flexible manipulator.

The robot configuration allows spherical rotation for flexible arm, which it can lead to couple between the transverse vibrations and it makes difficult for obtaining the optimal path. The simulation results (small and large models) compared to experimental result as shown in Fig. 11. The obtained optimal joint paths, corresponding to the minimum vibration are shown in Fig. 12. The oscillation amplitudes in the flexural responses of the system for the minimum vibration trajectory, has been reduced considerably.

As expected, the experimental results show that a significant reduction in manipulator vibration can be achieved by employing trajectory optimization. The optimization procedure improves the performance of the flexible arm in comparison with the fourth order trajectory. Figure 13 shows the tip position of the flexible arm in x, y and z coordinates. Also, it is observed that applying the proper input torque can decrease the tip vibration significantly. It means that for achieving a smoother path, minimum effort must be applied because of the inertia effects on the system.

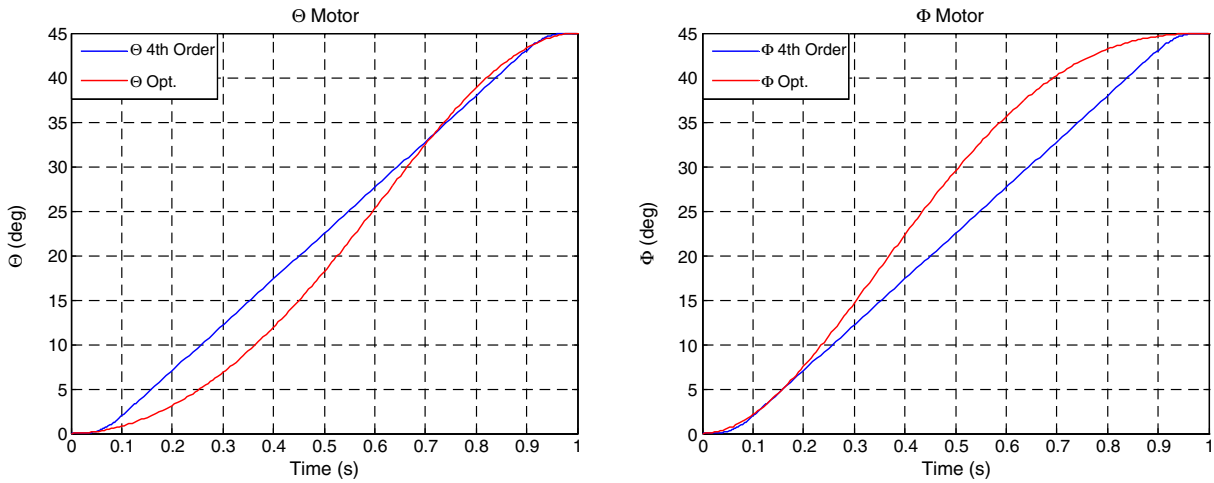

Fig. 12 The obtained optimal θ, ϕ and fourth order paths

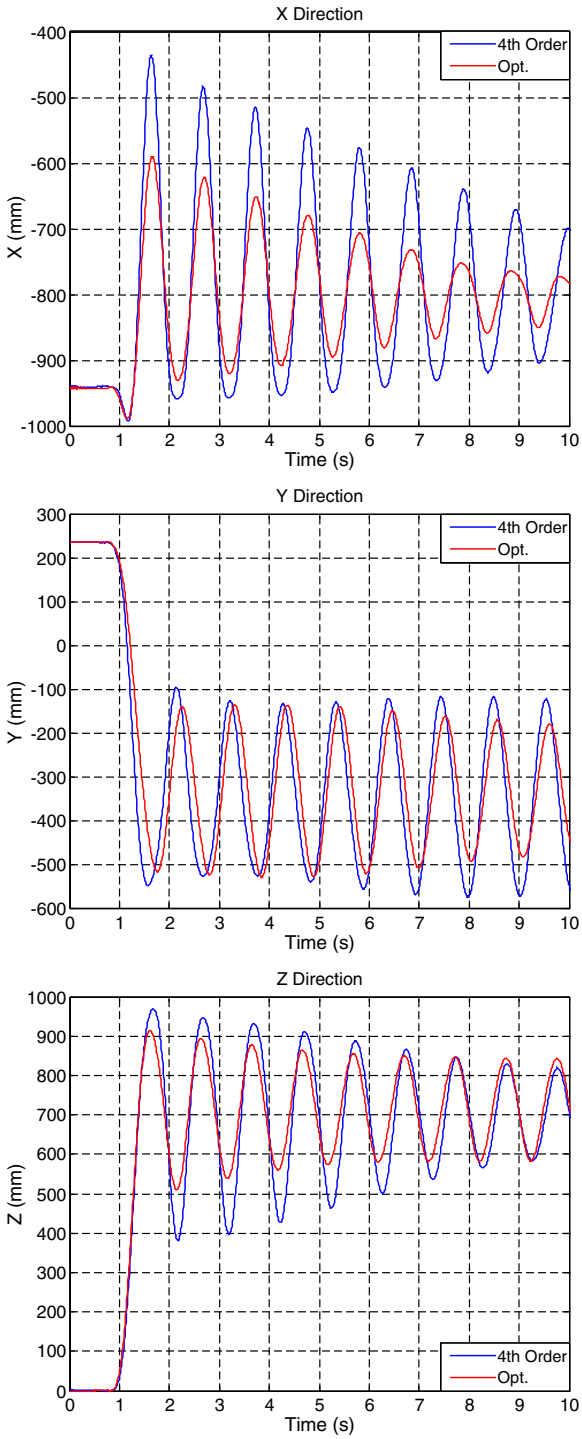

Fig. 13 The experimental results of the tip position in X, Y and Z directions, corresponding to the minimum vibration

6 Conclusions

In this paper, a new displacements approach is developed to determine the trajectory optimization for geometrically nonlinear flexible-link manipulators in point-to-point maneuver, based on the indirect solution of optimal control problem. The complete dynamic model using the combined Euler–Lagrange formulation and finite element method is derived, in which both the geometric elastic nonlinearity and the foreshortening effects are considered. This model leads to a constant stiffness matrix and makes the formulation particularly efficient in computational terms and numerically more stable than alternative geometrically nonlinear formulations based on lower-order terms. The Pontryagin's minimum principle is used to obtain the optimality conditions, which is lead to a standard form of a two-point boundary value problem. The proposed approach has been implemented and tested on a single-link very flexible arm and optimal paths with minimum effort and minimum vibration are studied. Through the use of the model, the obtained results are compared, both in simulation and experimentally, to a fourth-order polynomial trajectory designed in [26] in order to evaluate the results. The Numerical and experimental results indicate the effect of employing trajectory optimization in the performance improvement of the flexible manipulator. As it can be seen, the flexibility of link and adding the payload will increase the oscillation of torque curves and the amplitude of the vibrations. Finally, the minimum vibration problem is shown that applying the proper input torque can decrease the tip vibration significantly. Moreover by changing the penalty matrices values, various optimal trajectories with different specifications can be obtained which able the designer to select a suitable path through a set of obtained paths. The obtained results illustrate the power and efficiency of the model to overcome the high nonlinearity nature of the large deflection and optimization problem which with other methods may be very difficult or impossible. The optimal trajectory and corresponding input control obtained using this method can be used as a reference signal and feedforward command in control structure of flexible manipulators.

References

1. Yao, Y., Korayem, M.H., Basu, A.: Maximum allowable load of flexible manipulator for a given dynamic trajectory. Int. J. Robot. Comput. Integr. Manuf. **10**(4), 301–309 (1993)
2. Korayem, M.H., Heidari, A., Nikoobin, A.: Maximum allowable load of flexible mobile manipulators using finite element approach. Int. J. AMT **36**(10), 606–617 (2008)
3. Korayem, M.H., Heidari, A.: Effect of payload variation on the residual vibration of flexible manipulators at the end of the given path. Sci. Iran. **16**(4), 332–343 (2009)
4. Bakr, E.M.: Dynamic analysis of geometrically nonlinear robot manipulators. Nonlinear Dyn. **11**(4), 329–346 (1996)
5. Simo, J.C., Vu-Quoc, L.: The role of nonlinear theories in transient dynamic analysis of flexible structures. J. Sound Vib. **119**(1), 487–508 (1987)
6. Korayem, M.H., Yao, Y., Basu, A.: Application of symbolic manipulation to inverse dynamics and kinematics of elastic robot. Int. J. Adv. Manuf. Technol. **9**(5), 343–350 (1994)
7. Shaker, M.C., Ghosal, A.: Nonlinear modeling of flexible manipulators using non-dimensional variables. ASME J. Comput. Nonlinear Dyn. **1**(2), 123–134 (2006)
8. Korayem, M.H., Haghpanahi, M., Heidari, H.R.: Maximum allowable dynamic load of flexible manipulators undergoing large deformation. Sci. Iran. **17**(1), 61–74 (2010)
9. Damaren, C., Sharf, L.: Simulation of flexible-link manipulators with inertia and geometric nonlinearities. ASME J. Dyn. Syst. Meas. Control **117**(1), 74–87 (1995)
10. Mayo, J., Dominguez, J., Shabana, A.A.: Geometrically nonlinear formulations of beams in flexible multibody dynamics. ASME J. Vib. Acoust. **117**(4), 501–509 (1995)
11. Kane, T.R., Ryan, R.R., Banerjee, A.K.: Dynamics of a cantilever beam attached to a moving base. J. Guid. Control **10**(2), 139–151 (1987)
12. Absy, H.E.L., Shabana, A.A.: Geometric stiffness and stability of rigid body modes. J. Sound Vib. **207**(4), 465–496 (1997)
13. Omar, M.A., Shabana, A.A.: A two-dimensional shear deformable beam for large rotation and deformation problems. J. Sound Vib. **243**(3), 565–576 (2001)
14. Wang, C.Y.E., Timoszyk, W.K., Bobrow, J.E.: Payload maximization for open chained manipulator: finding weightlifting motions for a Puma 762 robot. IEEE Trans. Robot. Autom. **17**(2), 218–224 (2001)
15. Wilson, D.G., Robinett, R.D., Eisler, G.R.: Discrete dynamic programming for optimized path planning of flexible robots. IEEE Int. Conf. Intell. Robot. Syst. **3**(1), 2918–2923 (2004)
16. Korayem, M.H., Nikoobin, A.: Maximum load carrying capacity of mobile manipulators: optimal control approach. Robotica **27**(1), 147–159 (2009)
17. Mohri, A., Furuno, S., Yamamoto, M.: Trajectory planning of mobile manipulator with end-effector's specified path. IEEE Int. Conf. Intell. Robot. Syst. **4**(1), 2264–2269 (2001)
18. Park, K.J.: Trajectory flexible robot manipulator path design to reduce the endpoint residual vibration under torque constraints. J. Sound Vib. **275**(3), 1051–1068 (2004)
19. Benosman, M., Le Vey, G., Lanari, L., De Luca, A.: Rest-to-rest motion for planar multi-link flexible manipulator through backward recursion. Dyn. Syst. Meas. Control **126**(1), 115–123 (2004)
20. Szyszkowski, W., Youck, D., De Luca, A.: Optimal control of a flexible manipulator. J. Comput. Struct. **47**(4), 801–813 (1993)
21. Sarkar, P.K., Yamamoto, M., Mohri, A.: On the trajectory planning of a planar elastic manipulator under gravity. IEEE Trans. Robot. Autom. **15**(2), 357–362 (1999)
22. Kojima, H., Kibe, T.: Optimal trajectory planning of a two link flexible robot arm based on genetic algorithm for residual vibration reduction. IEEE Int. Conf. Intell. Robot. Syst. **4**(1), 2276–2281 (2001)
23. Sharf, I.: Geometrically non-linear beam element for dynamics of multibody systems. Int. J. Numer. Methods Eng. **39**(5), 763–783 (1996)
24. Shampine, L.F., Reichelt, M.W., Kierzenka, J.: Solving boundary value problems for ordinary differential equations in Matlab with bvp4c. Available from: http://www.mathworks.com/bvp tutorial (2000)
25. Wu, S.C., Haug, E.J.: Geometric non-linear substructuring for dynamic of flexible mechanical systems. Int. J. Numer. Methods Eng. **26**(10), 2211–2226 (1988)
26. Ramos, F., Feliu, V., Payo, I.: Design of trajectories with physical constraints for very lightweight single link flexible arms. J. Vib. Control **14**(8), 1091–1110 (2008)